LHC-B 97-008/LHCC
CERN/LHCC 97-14
February 21, 1997

Trigger and Data Acquisition System for the LHC-B Experiment

Current Status and Work Programme

The LHC-B Collaboration

Abstract

The trigger and data acquisition system is one of the most challenging aspects of the LHC-B experiment. The progress made on this subject since the submission of the Letter of Intent is summarised in this report. The work programme necessary to demonstrate the feasibility of the LHC-B trigger and data acquisition system is presented.

Contents

1 Introduction

At the LHC energies, the $\mathrm{b\overline{b}}$ cross section is estimated to be $\sigma_{\mathrm{b\overline{b}}} \approx 500\ \mu$b and the cross section ratio $\sigma_{\mathrm{b\overline{b}}}/\sigma_{\mathrm{inelastic}} \sim 5 \times 10^{-3}$, where $\sigma_{\mathrm{inelastic}}$ is the inelastic pp interaction cross section, which is dominated by the events with light quarks (u, d and s). We refer to these as "minimum bias" events in this paper. The bunch crossing rate of the LHC is 40 MHz, i.e. bunches are colliding every 25 ns at the interaction points.

The trigger system for an experiment studying b-quark physics at LHC must cope with this cross section ratio which is much smaller than those for $\mathrm{e^+e^-}$ B-meson factories and LEP experiments. The high bunch crossing rate requires that the trigger system at early levels must work at a very high rate and suppress the minimum bias events efficiently. The main goal for B physics studies at LHC is to measure CP violation parameters with high precision and to search for very rare decay modes and those forbidden in the standard model. The branching fractions for the relevant decay modes are very small, i.e. $\leq 10^{-5}$. In order to exploit the large $\mathrm{b\overline{b}}$ cross section at LHC, the trigger should select the desired b-hadron decay modes.

In the early levels of the LHC-B trigger system, the following features are to be used to distinguish events with b-hadrons from minimum bias events :

- Particles associated with the b-hadron decay have larger transverse momentum (p_{T}) on average than particles found in the minimum bias events, due to the large b-hadron mass and the transverse momentum distribution of the b-hadrons with respect to the proton beam direction.

- The b-hadron has a lifetime of $\sim$ 1 ps and decays most of the time into the c-hadron whose lifetime is also $\sim$ 1 ps. Therefore, several decay vertices are present in the event and tracks from these decay vertices have large impact parameters with respect to the interaction point (primary vertex).

Compared to the scheme proposed in the Letter of Intent (LoI) [1], determination of the decay vertices has now been moved into an earlier trigger level. Cuts applied in the trigger are optimised to select events useful for the off-line physics analysis.

Events with more than one pp interaction in the same bunch crossing are difficult to analyse, due to the increased particle multiplicities, and multiple primary vertices. Assuming a luminosity of 1.5×10^{32} cm^{-2} s^{-1}, there are on average 0.39 interactions per bunch crossing. Approximately 83% of all interactions occur in single-interaction crossings. It is planned to reject the remaining multiple-interaction events, and thus provide a "pile-up" veto, by measuring the total energy in the calorimeters in the first trigger level. In addition, the new vertex topology trigger should recognize multiple primary interaction vertices allowing an additional rejection capability.

In the higher levels of the trigger, B-mesons are reconstructed, at least partially, to select the decay final states which are relevant for the physics analysis.

In this document, we first describe the trigger scheme presented in the LoI. We also discuss the shortcomings of the LoI scheme which led us to the new trigger scheme. This

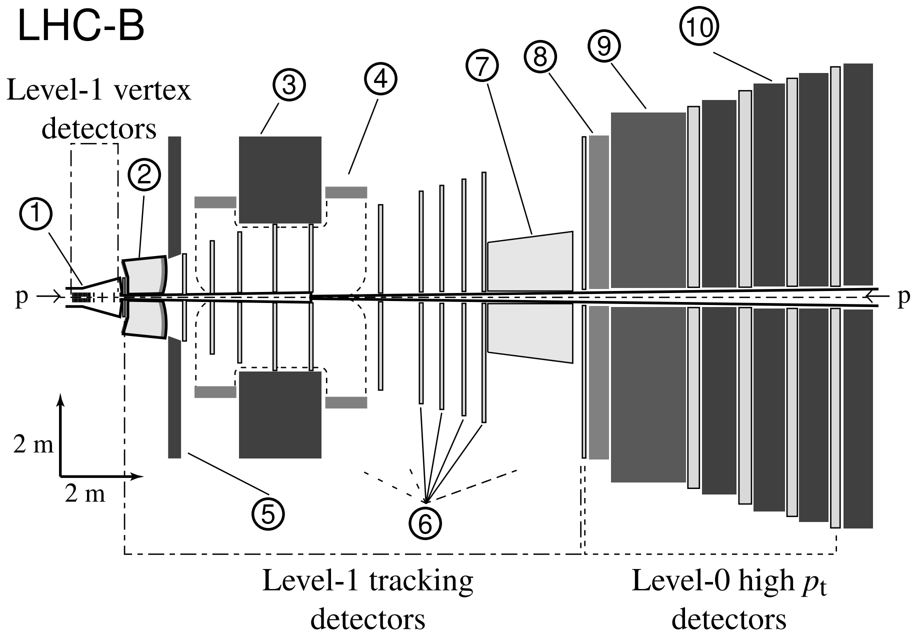

Figure 1: The LHC-B detector:1) Vertex detector, 2) RICH-1, 3) Magnet yoke, 4) Coil, 5) Magnet mirror plate, 6) Tracking system, 7) RICH-2, 8) Electromagnetic calorimeter, 9) Hadron calorimeter, 10) Muon system. The RICH systems are not used in the Level-0 and Level-1 triggers.

is followed by a description of the new trigger strategy. Finally we present the work programme we intend to carry out in order to be able to propose a feasible trigger system by the end of 1997, together with the list of people involved. More details of the trigger status can be found elsewhere [2].

2 The LoI Trigger Scheme

Fig. 1 shows a schematic view of the LHC-B detector. For the Letter of Intent (LoI), we considered a trigger scheme with three levels: The Level-1 trigger consisted of a combination of high-p_T electron, muon and hadron triggers. For the electron and hadron triggers, the calorimeter system consisting of preshower counter, electromagnetic and hadron calorimeters was used to select candidate tracks with large transverse energy. The muon trajectory was measured by the muon system. The p_T threshold values were tuned so that each trigger component gave a rejection factor of ~ 100 for minimum bias events. In addition, the pile-up veto is introduced to reject events with more than one pp interaction.

The Level-2 trigger consisted of tracking and vertex topology components. In the former, the trigger tracks found at Level-1 were reconstructed in the tracking detector and momenta were measured using the spectrometer magnetic field giving an improved

p_{T} resolution. In the latter, the silicon micro strip vertex detector was used to reject events which are compatible with having only one vertex. A combined rejection factor of ~ 20 was expected.

The Level-3 trigger involved the full reconstruction of the event using the full detector information. Events were selected based on the fully or partially reconstructed final states.

With the expected luminosity of 1.5×10^{32} cm^{-2}s^{-1}, the predicted Level-1 output rate was ~ 200 kHz in average. Therefore, the data would have to be transferred from the pipeline of the front-end detector electronics to the Level-2 buffer with a rate of ~ 200 kHz. This results in technical problems in reading out the detectors into the the data acquisition buffers, and also leads to high costs for the event building hardware and processing capability necessary to deal with this input rate to the data acquisition system.

In the LoI study, the trigger performance was not yet optimised to preferentially select the b-hadron events which are useful for the off-line physics analysis.

3 The New Trigger Concept

In the current trigger strategy, we have four levels of triggering. Level-0 consists of the high-p_{T} trigger similar to the Level-1 trigger of the LoI. In Level-1, the tracking and vertex topology triggers are executed in custom-built electronics while the data are still stored in the front-end electronics. After the Level-1 decision, the data are transferred from the front-end electronics to the Level-2 data acquisition buffers. The rate for this data transfer is substantially less than that assumed in the LoI. The Level-2 and Level-3 algorithms are executed in processors using the data from these buffers. The data flow for this new scheme is shown in Fig. 2, and the functionality of the four trigger levels can be summarised as follows:

Level-0

This consists of the high-p_{T} electron, hadron and muon triggers implemented in custom-built hardware and fully pipelined at 40 MHz with a fixed latency of 3.2 μs. The data from all bunch crossings are stored in pipelines, and passed to the Level-1 buffers implemented in the front-end electronics, when a positive decision is given by the Level-0 trigger. The aim is to produce an average input trigger rate to Level-1 of 1 MHz.

Level-1

Level-1 is based on the track and vertex topology triggers implemented in custom built hardware running with an average input rate of ~ 1 MHz and a variable latency of the order of 50 μs. In the track trigger, the high-p_{T} hadron, electron and muon candidates found by the Level-0 trigger are used as seeds to find corresponding tracks in the spectrometer. The high-p_{T} candidates are validated and their momenta are measured with a better accuracy, thus allowing an improved p_{T} cut. In addition tracks not originating from the nominal interaction region (e.g. photon conversions) can be suppressed.

In the vertex topology trigger, the first step is to determine the primary vertex. Cur-

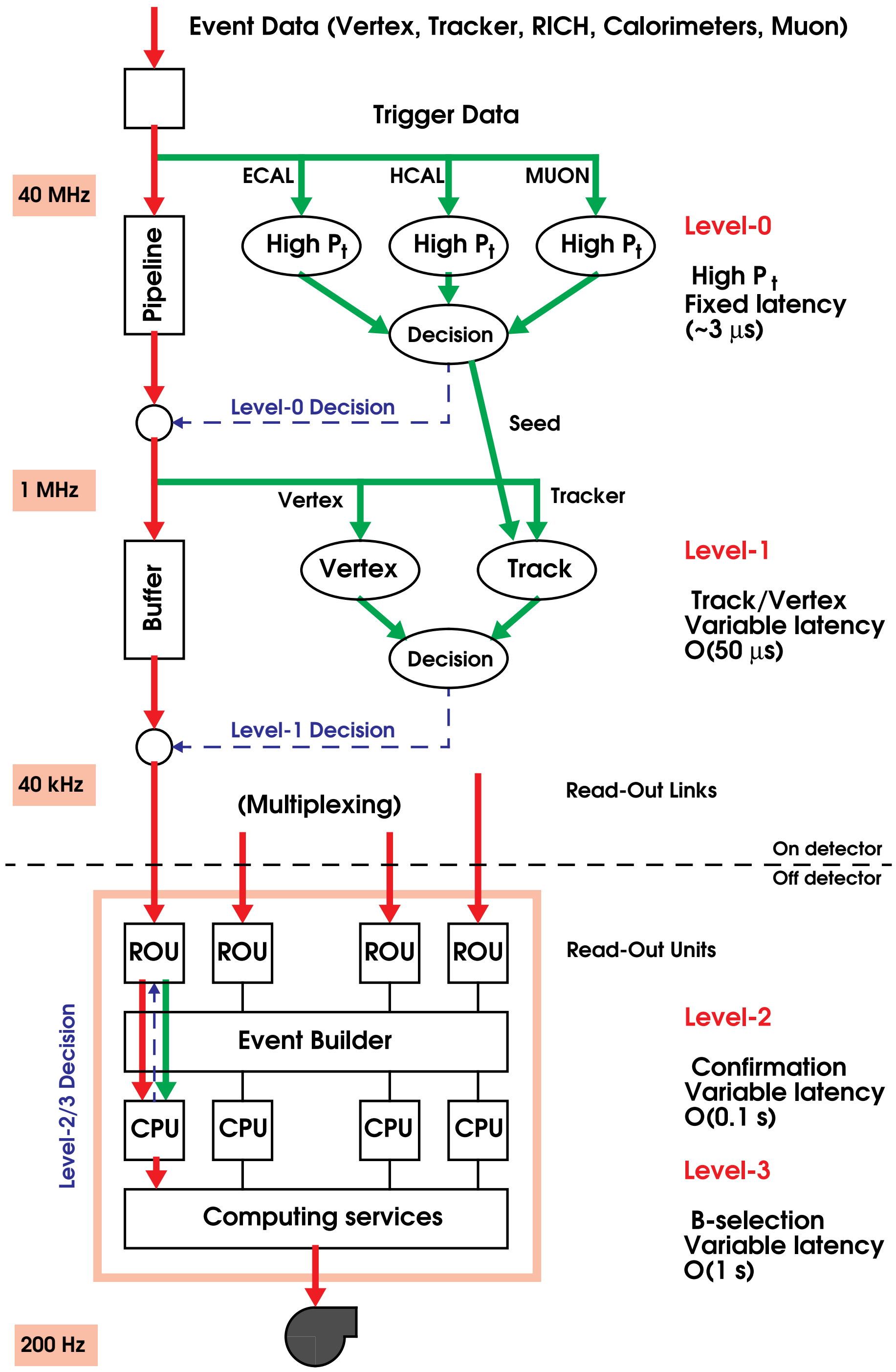

Figure 2: Trigger scheme and data flow.

rently, two different approaches are being studied. One is to install a special purpose silicon detector parallel to the beam direction at the interaction point detecting tracks in the central region. The other approach uses the LHC-B vertex detector which finds all the tracks within the spectrometer acceptance. In the second step, tracks with large impact parameters with respect to the primary vertex are selected. After reconstructing these selected tracks in space, each of them is combined with all the other tracks to form a two-track vertex. This trigger is tuned to accept b-hadron events where the b-hadrons decay some distance from the primary vertex. Similar cuts are imposed in the off-line physics analysis in order to reduce the combinatorial backgrounds.

Positive decisions at this level initiate the readout of the data from the front-end electronics into the Level-2 data acquisition buffers, with an expected rate of ~ 40 kHz.

Level-2

In the Level-2 trigger, we intend to refine the high p_{T} tracks and decay vertices found in Level-0 and Level-1. This is done by combining the data from the vertex detector and the spectrometer tracking devices using the full resolution of the detector. Cuts based on the refined information reduce the rate of events required for the Level-3 processing to ~ 5 kHz.

Level-3

The Level-3 trigger uses full detector information and reconstructs fully or partially the final states of B and D meson decays. The output of the trigger is recorded with a rate of ~ 200 Hz.

This scheme leads to reduced costs for the data acquisition system as a consequence of the reduced rate into Level-2. The lower p_{T} thresholds allowed in the Level-0 triggers, due to the implementation of hardware tracking/vertex triggers, should also give a higher yield of physics with respect to the LoI proposal.

4 High Transverse Momentum Trigger - Level-0

Since the new trigger scheme requires a suppression by a factor of only 10 for minimum bias events, Level-0 trigger strategies can be simplified compared with those considered in the LoI. Fig. 1 also indicates the detector components now used for the Level-0 trigger. Compared to the LoI scheme, the pad chamber after the magnet is removed and we are currently also considering whether the preshower counter is necessary. Preliminary studies show that the preshower counter is not needed for high-p_{T} (electron and hadron) Level-0 triggers. In this section, we summarize the results from the high-p_{T} hadron, electron and muon trigger studies made after the submission of the LoI. Details can be found in various LHC-B notes [3, 4, 5, 6].

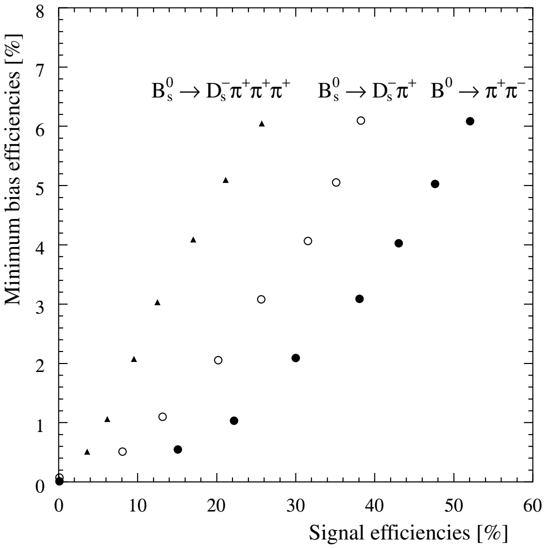

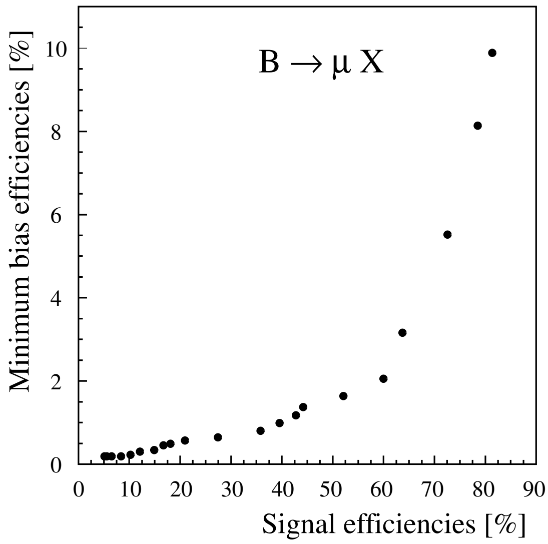

Figure 3: The efficiencies of the high-p_T hadron trigger for minimum bias events as a function of the trigger efficiencies for b-hadron events with $B^0 \to \pi^+\pi^-$, $B_s \to D_s^-(\to K^+K^-\pi^-)\pi^+$ and $B_s \to D_s^-(\to K^+K^-\pi^-)\pi^+\pi^+\pi^-$ decays. Efficiencies are normalized to those events where all the B decay tracks are detected in the LHC-B spectrometer.

Figure 4: The efficiency of the high-p_T muon trigger for minimum bias events as a function of the trigger efficiency for b-hadron events with muons from semileptonic B-meson decays. The efficiency for the b-hadron events is calculated for those events where the muon is in the acceptance of the LHC-B detector.

4.1 Electron and hadron trigger

Fig. 3 demonstrates the simulated performance of the high-p_T hadron trigger where the trigger efficiencies for minimum bias events are plotted as a function of efficiencies for three different types of b-hadron events, where the following decay modes are present; $B^0 \to \pi^+\pi^-$, $B_s \to D_s^-(\to K^+K^-\pi^-)\pi^+$ and $B_s \to D_s^-(\to K^+K^-\pi^-)\pi^+\pi^+\pi^-$ respectively. The first decay mode represents final states with two high momentum particles where the high-p_T hadron trigger is very effective. In the second decay mode, only one particle in the final state has a high momentum and the trigger becomes less effective. There is no high momentum particle in the last decay mode. The trigger efficiency for this event type is still higher than that for minimum bias events. The trigger efficiencies are calculated for those events where all the tracks from the B-meson are detected in the LHC-B spectrometer.

The following conclusions have been drawn from the studies on the calorimeters and the Level-0 trigger performance :

- In the very forward region of the spectrometer, i.e. θ = 10-30 mrad where θ is the polar angle with respect to the beam axis, the particle densities are very high, mainly due to hadrons, and can produce a high-p_T hadron signature from overlapping particles in the calorimeter. It has been shown [3] that the yield of useful b-hadron events increases by excluding the calorimeter below 30 mrad for the high-p_T hadron trigger. For the electron trigger this results in a signal loss of only a few percent. This region is subject to severe radiation problems, and would be very costly to build.

- The energy resolution and granularity of the calorimeters required by the high-p_T trigger are being studied with full GEANT simulation, which also examines the validity of the shower parameterization used in the fast simulation program. Studies based on the parameterized showers show that the high-p_T hadron trigger requires only a modest energy resolution of $(100/\sqrt{E} \oplus 10)\%$ for the hadron calorimeter.

The majority of minimum bias events passing the high-p_T electron trigger are triggered by the electrons with real high-p_T, originating from photon conversion along the spectrometer. Therefore the Level-1 tracking trigger could provide an additional rejection factor of ~ 3 for minimum bias events.

Minimum bias events passing the hadron trigger are mainly due to real high-p_T hadrons originating from the interaction point. Therefore the Level-1 tracking trigger with an improved momentum measurement can reject the minimum bias events by at most a factor of ~ 2.

4.2 Muon trigger

The algorithm for the high-p_T muon trigger is simplified using only the four chamber stations in the muon system after the calorimeters and one in front of the calorimeter system. The three dimensional field map, calculated for the proposed dipole magnet of the spectrometer, is used in the simulation. It has also been shown that the requirement on the homogeneity of the magnetic field can be relaxed, i.e. increasing the field component of the non-bending plane by a factor of two with respect to the original design does not degrade the performance of the trigger.

The background muon density in the very forward direction is still low even including all the secondary interactions of particles in the beam pipe and other detector material. Therefore, it is preferable to place the muon system as close to the beam as possible. On the other hand, the flux of charged tracks in the muon chamber system for small θ is high, due to the background produced by the interactions of primary particles in the beam pipe, calorimeters and muon shields. This increases the occupancy of the chamber stations in this region. Studies are in progress which optimize the minimum polar angle of the detector by calculating all the background particles coming from the detector components, beam pipe and shielding.

By scaling the results obtained for the CMS experiment, it is estimated that the muon background produced by the LHC machine introduces an increase of the muon high-p_T trigger rate of less than 15%.

The granularity required for the muon stations is also under study. The first results show that a large number of channels, of order 150 k, are required.

Fig. 4 shows the simulation result of the trigger efficiency for minimum bias events as a function of the efficiency for b-hadron events which include the inclusive semileptonic B-meson decay to a muon. The efficiency of the b-hadron events is calculated for those events where the muon is in the detector acceptance.

4.3 Planned further studies

Our plans for 1997 are

- Update the simulation software to include the latest detector geometry and trigger algorithms.
- Study the performance of the high p_{T} triggers with varying parameters.
- Investigate how the Level-0 bandwidth can be divided between the components so as to optimise the physics yield.
- Perform an implementation study of the Level-0 trigger using the 3D-Flow [7] hardware as a model for implementing and testing algorithms. This will include beam tests possibly commencing in late 1997, and continuing in 1998.

5 Tracking Trigger

There are three functions proposed for the tracking trigger :

- Validation of the Level-0 high p_{T} candidates by searching for the corresponding track in the upstream chambers. All Level-0 trigger clusters with p_{T} above a given threshold are validated.
- A more precise p_{T} cut using the extra track information.
- Rejection of tracks which do not come from the interaction region. In order to apply effective cuts tracking is continued upstream through the tracking stations in the magnet.

The algorithm being developed is similar to that used for the HERA-B [8] first level trigger. It is proposed to vary the station granularity in relation to the expected occupancy. A track search is started by a seed from one of the three high p_{T} triggers, with this seed being extrapolated to the closest tracking station.

Track candidates are then moved from plane to plane, updating the precision of predictions as more information is gathered. Linear predictions are used in the non-bending plane. In the bending plane, the prediction uses track curvature information once it has obtained the first five points.

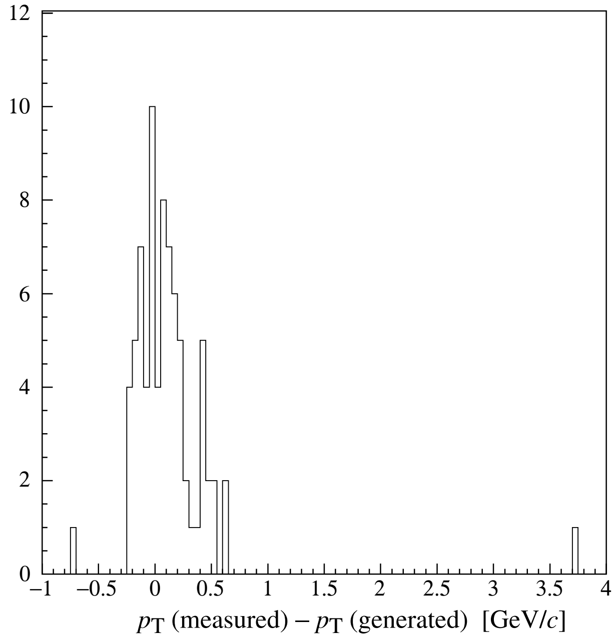

Figure 5: Difference between $p_{\rm T}$ [GeV/c] achieved with a medium granularity tracking trigger and the true $p_{\rm T}$

5.1 Required granularity of tracking chambers

Simulation studies have been performed on the granularity in the tracking stations required for pattern recognition and momentum determination. High $p_{\rm T}$ hadron trigger candidates were selected as follows:

- The transverse momentum of the track, as determined by the hadron trigger, is above 1 GeV/c.
- The track is a primary charged pion or kaon.
- The polar angle at the track origin is larger than 30 mrad, and the track origin is within 10 cm of the nominal interaction region.

Digitisation was performed in the framework of GEANT providing points for each tracking chamber. A stereo angle of 100 mrad was assumed, giving rise to a resolution about 10 times larger in y than in x.

Table 1 shows how the resolution and the pattern recognition deteriorates with resolution. Fig. 5 illustrates the momentum resolution achievable with the medium granularity. Chamber inefficiencies have been not taken into account. However it is expected that allowing one missing hit will compensate for the chamber inefficiencies. The incorrectly found tracks shown in the table are due to pattern recognition errors in a high density hit environment.

Table 1: Tracking performance for different granularities used in the trigger algorithm. Tracking stations are numbered as in the LoI. The p_T resolution is given in units of root mean square (σ) as well as the region in which 90% of the tracks are contained (last column)

granularity [cm] of tracking station No.				percentage of correct tracks found up to		p_T resolution [GeV/c]	
	13-9	8-4	3-1	station 8	station 1	σ	90%
coarse	1.0	0.5	0.25			0.55	1.6
medium	0.5	0.25	0.125	98%	87%	0.32	0.75
fine	0.25	0.125	0.0625	98%	86%	0.12	0.67

5.2 Hardware implementation

For a first implementation study it has been assumed that the track finding hardware is situated on the tracking chamber stations themselves, and thus close to the front-end readout electronics.

The two coarsest granularities shown in Table 1 can be realised directly with the wire signals of the honeycomb tracking chambers. A 0.3 cm granularity could be realised by ORing the wires of two (staggered) planes of honeycomb chambers.

For finer granularities a drift time analysis has to be performed. A possible solution is that proposed for the ATLAS TRT detector [9]. On two adjacent wire planes, the sum of the drift times is required to be a constant in order to reduce ghost hits. The difference of the two drift times gives the hit coordinate.

The tracking electronics receives track candidates together with the estimated hit coordinates for this chamber station. It finds hits matching the prediction, makes a new prediction for the next station, updates the track candidate information and passes it to the corresponding region of the next tracking station. With an average Level-0 trigger rate of 1 MHz there are 40 cycles at 40 MHz available for the computation. This type of "local" algorithm is well suited to be implemented in a pipelined and distributed processing system.

5.3 Planned further studies

- Integrate the tracking trigger algorithm into the simulation software.
- Study the performance of the tracking trigger algorithm for acceptance of physics channels and rejection of background.
- Continue implementation studies for the tracking electronics based on the HERA-B design.

6 Vertex Topology Trigger

The strategy employed for the vertex trigger is first to measure the primary vertex, and then look for secondary vertices at a distance from the primary vertex compatible with B decay lengths. The operation of the secondary track and vertex finding algorithm can be greatly simplified if the main silicon detectors follow an r-ϕ geometry (see Section 6.1). This geometry has the additional advantage of a more flexible design with respect to the optimisation of the algorithms. Thus, for example, the strip pitches can be adapted to the resolution and occupancy requirements, which vary mainly as a function of the radius. The r-ϕ geometry allows the division of the track finding into independent, parallel computations for the separate ϕ sectors.

The algorithm can be decomposed into the following phases :

1. **Track Segment and Primary Vertex Finding**

   In the first phase only the r-information is used to reconstruct straight tracks in each ϕ-sector separately. These tracks can then be used to calculate a primary vertex using a histogramming technique.

2. **2-D Impact Parameter cut**

   A cut is now made on the impact parameter of tracks with respect to the computed primary vertex. In order to proceed to the next stage a sufficient number of tracks must pass this cut.

3. **3-D Track Segments and Secondary Vertices**

   The ϕ-information is added to the surviving track candidates in order to reconstruct tracks in three dimensions. Finally, the secondary vertex reconstruction uses all combinations of two tracks which are close in space and which have large impact parameters. This reduces the number of combinations and yields a high minimum bias rejection.

6.1 Layout of the r-ϕ silicon vertex detector

The LoI layout in z for the silicon stations ensures that every track coming from either the primary or a secondary vertex, and which is within the spectrometer acceptance, hits at least two planes of the vertex detector. A vertex detector station consists of 6 ϕ sectors (60°), each with two planes for r and ϕ measurements respectively.

The r sensitive detector plane has strips at constant radius, starting at 1 cm distance from the beam and going up to 6 cm, with strip pitches of 40, 60 and 80 μm (see Fig. 6). This allows a simple conversion from strip numbers to r-coordinates. The division into inner, middle and outer sections is motivated by the fact that any track inside the spectrometer acceptance hits the silicon detectors at least once at a radius $r < 2.5$ cm, and also because the measurement accuracy of these first points have a major effect on the resolution of the z coordinate of the vertex position. The inner section is further divided into two 30° sectors in order to make the track finding simpler by avoiding hit ambiguities.

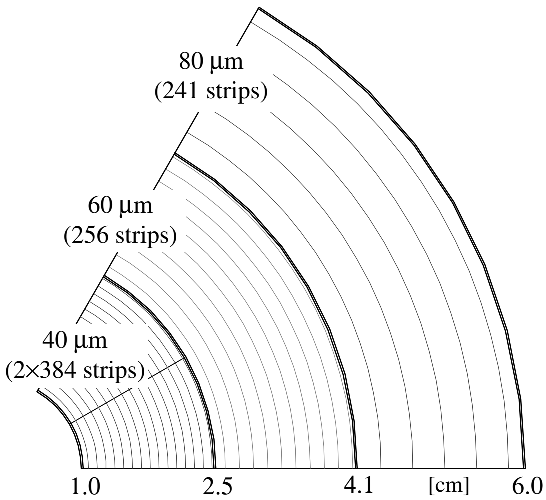

Figure 6: Schematic drawing of one r-detector.

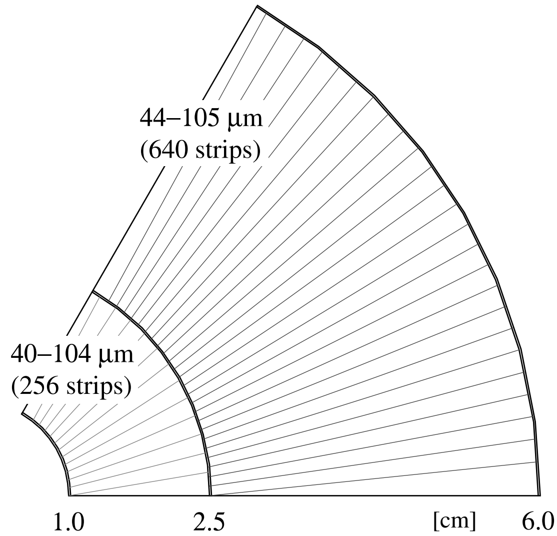

Figure 7: Schematic drawing of one ϕ-detector.

The ϕ coordinates of a track are measured by silicon detectors with strips arranged almost radially (see Fig. 7). The strips are tilted by a small angle ($\pm 5°$) for consecutive stations, in order to resolve ambiguities when combining the r and ϕ information. Strip pitches range from 40 μm to 100 μm.

6.2 Track finding algorithm

Tracks are reconstructed firstly in the r-projection. The hit map of three successive planes of the same ϕ sector is sent to one hardware processor. The hits in the inner part of station i (1 cm$< r <$ 2.5 cm) are combined with the hits of station $i+1$ (1 cm$< r <$ 4.1 cm) to define straight lines. A track is confirmed by a hit at the extrapolated position in station $i+2$. A stringent collinearity cut can be used to reject low momentum tracks due to their multiple scattering. Fig. 8 shows an extrapolation resolution of 35 μm for particles with momenta greater than 10 GeV/c.

Several segments of the same track could be found in different 3-hit hardware processors. Thus a rejection process will be necessary to remove duplicate segments, leaving the segment with a hit closest to the beam.

6.3 Primary vertex computation

The primary vertex z coordinate is computed by histogramming the z-coordinates of two-track vertices in 200 μm bins. Combinations are made of tracks from opposite (± 2) ϕ-sectors. On average, about 150 two track combinations exist in one event, but less than 50 are sufficient for the desired precision. The bin with the maximum number of

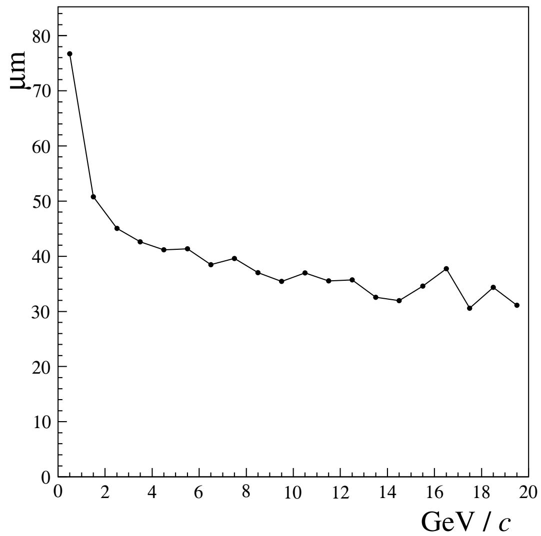

Figure 8: Average extrapolation error in the third station as a function of particle momenta

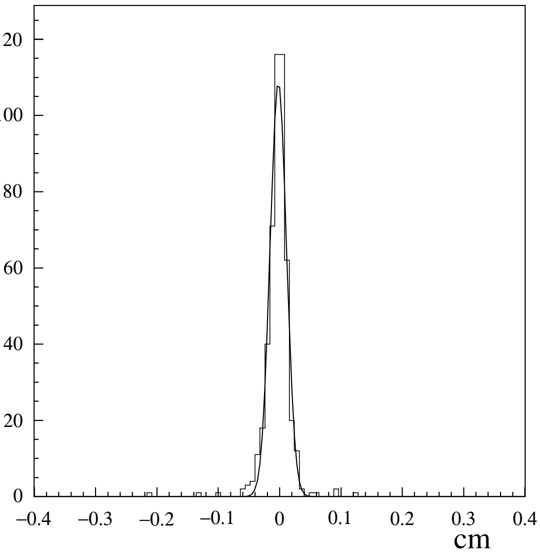

Figure 9: Resolution of the z-coordinate of the primary vertex

combinations defines the z-position of the primary vertex with a resolution of 150 μm (Fig. 9). A more refined procedure using the weighted average of the maximum bin and its two neighbours would give a resolution of 120 μm. In addition, some crude information about the transverse position of the primary vertex is obtained.

The primary vertex computation described above uses the standard silicon detector planes. Investigations are also proceeding on the possible application of a special barrel silicon detector to aid in the fast computation of the primary vertex.

Fig. 10 shows a possible geometry for this special barrel silicon detector. There are two layers of strip detectors in y-z planes at each side of the beam. The strips lie in y perpendicular to the beam direction. The strip pitches in the two layers are chosen such that their ratio is equal to the ratio of the distance of the two layers from the beam line.

Given the small transverse dimensions of the beam, this projective geometry leads to a simple relationship between the hit coordinates for tracks emanating from the interaction point and the z coordinate of the interaction point. The z-position of the primary vertex is directly proportional to the difference of the indices of the strip hits in the two layers, for an event track which traverses the two layers.

The performance of such a barrel detector has been simulated, using the standard LHC-B full GEANT simulation, and PYTHIA generated $b\overline{b}$-events. Two silicon strip layers were added to the LHC-B lay-out, centred around the interaction volume, at distances of 5 and 10 cm to the beam direction, and with strip pitches of 100 and 200 μm respectively. The results demonstrate that histogramming the difference for all hit combinations, followed by finding the histogram bin with the maximum number of entries, determines the primary vertex longitudinal position with an accuracy of the order of

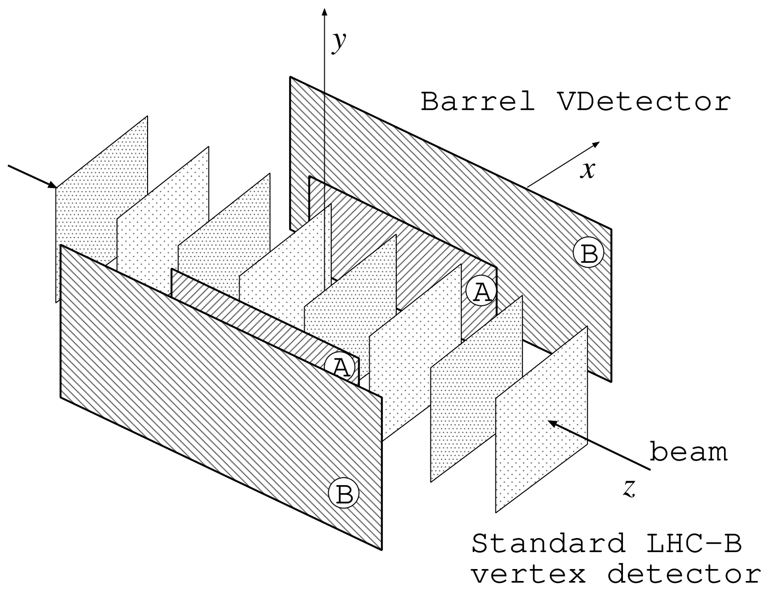

Figure 10: Layout of the barrel section as primary vertex detector

150 μm. Detector optimisation is being studied, and first ideas are being developed for hardware implementation using FPGAs or customized gate-arrays [10].

6.4 2-D impact parameter cut

As a prerequisite for the 3-D track analysis, a minimal number of tracks with large impact parameter to the primary vertex is required. This filter must reject minimum bias events while keeping a high efficiency for B events. Requiring at least one track with an impact parameter to the primary vertex of 4σ, and in addition, at least one with 2σ, results in a minimum bias retention of 39%, without losing any B-events.

Pile-up events, which have two separated primary vertices, could be rejected here by requiring less than a maximum number of tracks with a large impact parameter.

6.5 3-D track reconstruction

For the events surviving the 2-D impact parameter cut, the ϕ hit information of stations i and $i+1$ is now added to the track segments already found in the r projection with a large impact parameter. The extrapolation to station $i+2$, and the fact that the ϕ strips are rotated by a small angle, resolves any ambiguities.

6.6 Secondary vertex computation

The algorithm aims to find vertices which are separated significantly from the primary vertex. Since the momentum of the tracks is unknown, the error estimation of the im-

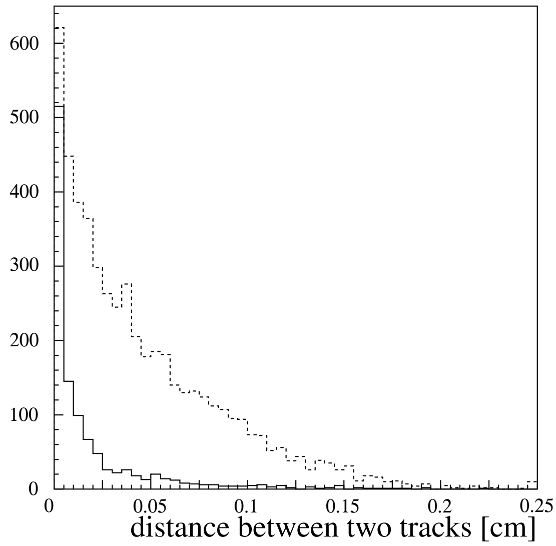

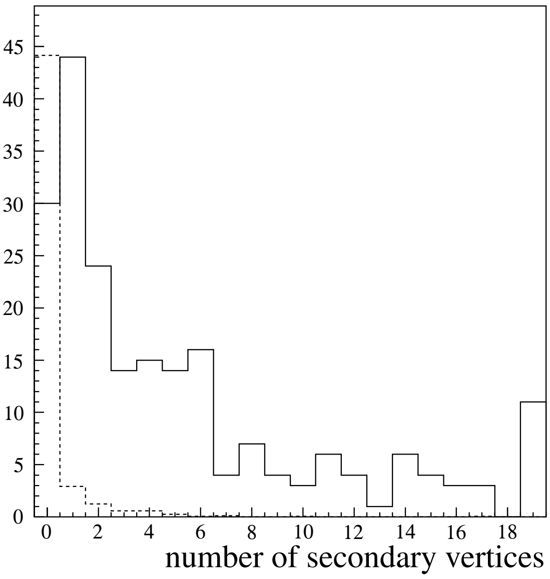

Figure 11: The closest distance in space between a track and any other track in the event is shown for tracks originating from a B (solid line) and for tracks in minimum bias events (dashed line)

Figure 12: The number of secondary 2-track vertices with a distance to the primary vertex larger than 5σ is shown for $B \to \pi\pi$ events (solid line) and for minimum bias events (dashed line)

pact parameters is derived from purely geometrical considerations, and assuming straight tracks.

Only 3D-tracks with an impact parameter (IP) less than 2 mm are considered. Also, in order to minimize the number of 2-track combinations considered, secondary vertices are constructed only if one of the two tracks has $IP/\sigma(IP) > 4$, and the other track has $IP/\sigma(IP) > 2$.

This leads to about 13 combinations on average for minimum bias events. Fig. 11 shows histograms for the closest distance in space between a track and any other track in the event for tracks originating from a B (solid line) and for tracks in minimum bias events (dashed line). Only vertices with a distance between tracks smaller than 250 μm are accepted. Fig. 12 shows the number of secondary 2-track vertices with a distance to the primary vertex larger than 5σ, for $B \to \pi\pi$ events (solid line) and for minimum bias events (dashed line).

6.7 Simulation results

The Level-1 trigger algorithm is being tailored to meet the selection criteria proposed for use off-line in the reconstruction of B-mesons. The decay mode $B \to \pi\pi$ is being used to demonstrate its performance, since this is one of the most demanding modes due to its low final state multiplicity and the absence of sub-mass constraints. The $B \to \pi\pi$ decay mode has a vertex with only two charged particles, and hence only two tracks will be required per vertex. However using the associated B-meson decay more than one vertex can be demanded per event in order to improve the suppression of minimum bias events.

Intersecting tracks with a plane perpendicular to the beam at the position of the primary vertex gives an error on the determination of the x and y position of the primary vertex of 25 μm. 200 μm is assumed for the error in the z-position of the primary vertex.

The B-mesons which decay to $\pi\pi$ or $D_s\pi\pi\pi$ have been generated within a cone of 600 mrad around the beam-axis, and all events have passed the Level-0 trigger conditions with cuts as defined in the LoI. The cuts have been tuned such that the Level-0 trigger accepts 2.4% of the minimum bias events, and 12% (7%) of the $B \rightarrow \pi\pi$ ($D_s\pi\pi\pi$) events.

In order to evaluate how well the vertex trigger performs for B events which can be reconstructed off-line, the B-events which passed the Level-0 trigger have been subjected to the following off-line cuts:

- The $B \rightarrow \pi\pi$ ($D_s\pi\pi\pi$) has a decay length larger than 1.5(0.5) mm.
- Both the pions from $B \rightarrow \pi\pi$ and at least three decay particles of $B_s \rightarrow D_s\pi\pi\pi$ are measured in at least three silicon stations, and have a momentum measurement from the spectrometer.
- $IP/\sigma(IP) > 3$ for both pions in the $B \rightarrow \pi\pi$ decay.

After these cuts, 30% (19%) of the $B \rightarrow \pi\pi$ ($D_s\pi\pi\pi$) events which passed the Level-0 trigger remain.

By varying the cut on the distance between primary and secondary vertices, (see Fig. 11), and on the the number of secondary vertices, (Fig. 12), the trigger efficiency can be determined as a function of the retention of minimum bias events (Fig. 13). As expected, choosing the cuts for a high efficiency of $B \rightarrow \pi\pi$ events gives a higher retention of minimum bias events compared to $B_s \rightarrow D_s\pi\pi\pi$. A 10% minimum bias retention is achieved together with an 75% efficiency for $B \rightarrow \pi\pi\dot{B}$y comparison, the acceptance was 38% for the topology trigger as described in the LoI, with the same minimum bias retention. With the new strategy a minimum bias retention of less than 3% gives a $B \rightarrow \pi\pi$ efficiency of more than 60%.

6.8 First ideas about trigger implementation

A critical issue for the realisation of the vertex trigger is the reading of the data from the silicon detector at 1 MHz. The feasibility of this is part of our future study programme. In addition we have begun a detailed study to investigate the feasibility of implementing the overall vertex topology trigger. A detailed report is available [11].

In the feasibility model silicon strips are read out with radiation hard chips, similar to the SCTB chips, which group 128 channels and include a digital pipeline for a binary hit readout after a positive Level-0 decision. The hits of the r-strips are compressed into addresses using priority encoders, and routed via parallel optical links to FPGAs which

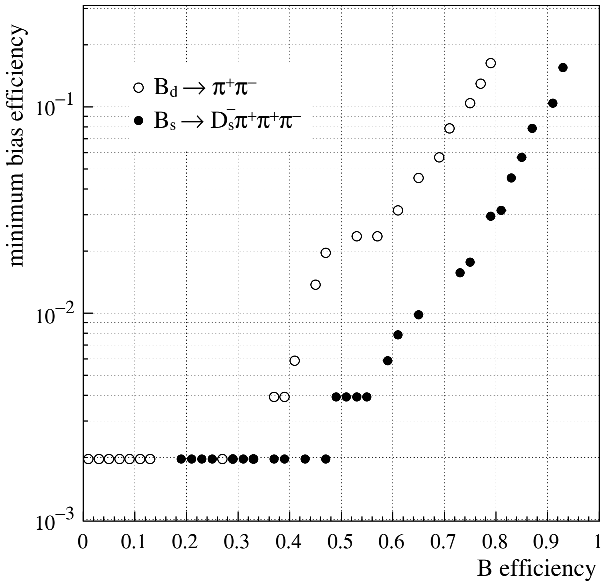

Figure 13: The retention of minimum bias events against the trigger efficiency of $B \to \pi\pi$ events (open circles) and $B_s \to D_s\pi\pi\pi$ events (closed circles).

perform the 2-D track triplet processing. In this model the 3-D processing would be performed by an array of programmable processors linked via high bandwidth links with 1 μs latency. These processors perform vertex finding using histogramming techniques.

The computation associated with the vertex trigger proceeds in an asynchronous manner. The target for the average computation time is 50 μs, and the implementation studies indicate that this could be achievable.

6.9 Planned further studies

- Integrate the vertex trigger algorithm into the simulation software.
- Study the performance of the vertex trigger for physics acceptance and background rejection. Tune the algorithms and the detector geometry.
- The r-ϕ detector performance will be evaluated. In particular signal to noise ratio at 40 MHz, the common mode, cross talk, cluster size, and the dynamic range needed for the digital conversion. We plan to setup a system for testing several detectors with r-ϕ geometry. Lab and beam tests are foreseen for 1997 and 1998.
- The environmental problems for the on-detector electronics will be evaluated. In particular we will study the power dissipation and cooling in the vacuum, electrical connections from the on-detector electronics to the outside world (feed-throughs), and expected radiation levels.

- Studies will be done on the readout of the silicon detector for the trigger at a rate of 1 MHz.
- The implementation study of the vertex topology trigger will be continued, based on optical couplers for detector readout to FPGAs, and processing with farm of processors connected by very high bandwidth links.

7 Data Acquisition Data flow and High Level Triggering

The Data Acquisition (DAQ) consists of the transfer of the detector data from the Front-End (FE) electronics to the data store. We are constructing a logical model for the FE electronics for all detectors in LHC-B based on our particular requirements for the Level-0/Level-1 trigger scheme. Data will be moved from the FE electronics to an intermediate buffer and afterwards the event fragments from these buffers will be assembled to form the complete event belonging to one trigger. The high-level trigger algorithms will run in processors accessing these event data.

7.1 Common front-end logical model

A general logical model for the FE electronics for all detectors has been developed. This is shown in Fig. 14. This model serves the purpose of guiding the analysis of the detector readout requirements and eventually could lead to a common FE chip design. The general model consists of a detector specific analog interface and data paths to the Level-0 and Level-1 trigger systems. The common parts are the Level-0 pipeline, the Level-1 buffer, the logic to deal with the trigger decisions, an interface for driving the readout and the interfaces to the control systems.

It should be noted that because of our Level-0/Level-1 triggering scheme the existing front-end designs, developed in the context of the LHC R&D programme, cannot be used directly in LHC-B. Therefore some effort is necessary in order to modify the existing designs to meet our requirements. This also includes the interface to, and the usage of, the trigger, timing and control distribution system (RD12/TTC) [13].

7.2 Event-building

Work is being undertaken in order to understand the requirements on the DAQ system in view of the new Level-0/Level-1 triggering scheme (see also Table 3).

Table 2 summarises the number of detector channels and their estimated occupancy. It can be seen that the average event size is approximately 80 Kbytes.

The estimated Level-1 accept rate is 40 kHz. Hence the total event building bandwidth required, after intermediate buffering, is of the order of 3 Gbytes/s in the worst case, i.e. if all the event data is transferred at the rate of the Level-1 triggers. More sophisticated

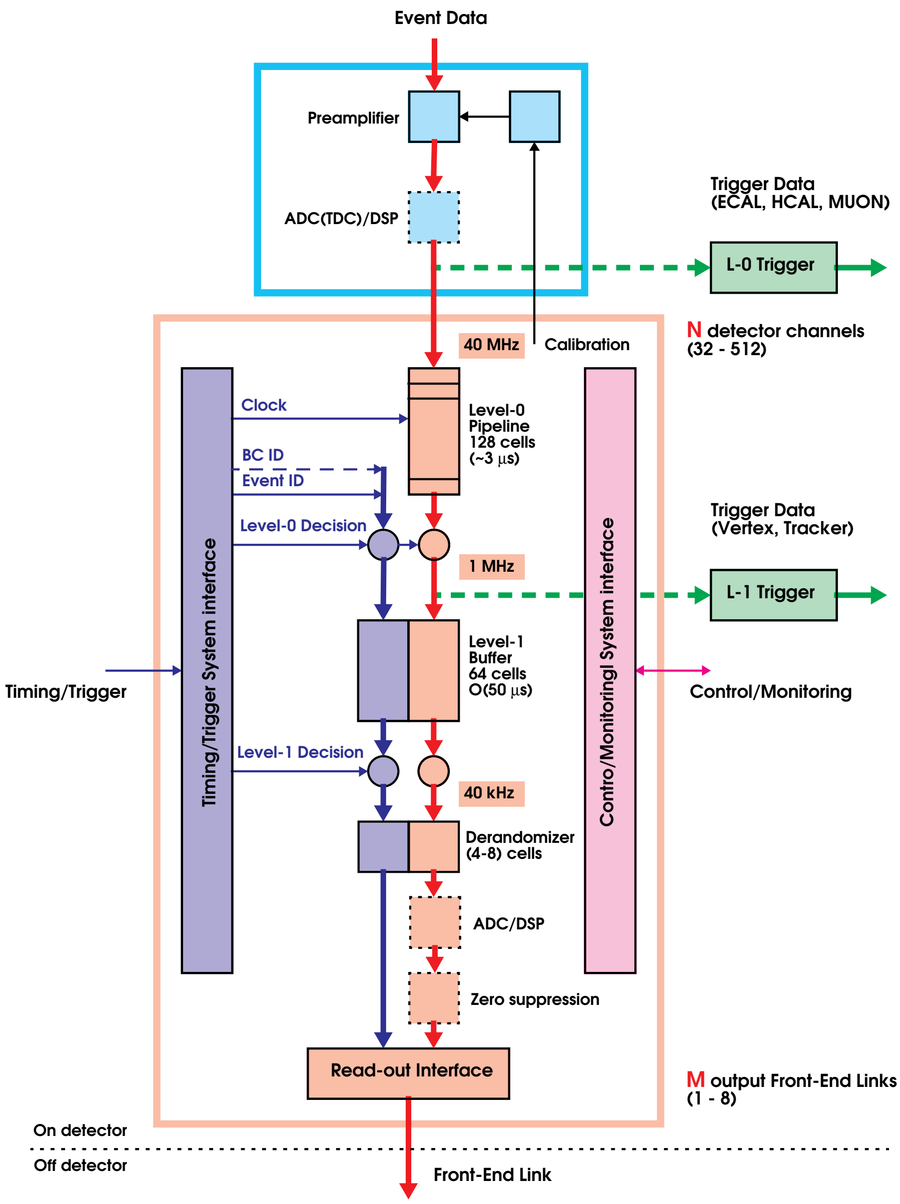

Figure 14: Logical model for the front end electronics

Table 2: Number of detector channels and estimated occupancies

Detector	Channels (k)	Occupancy per cent	Event Size Kbyte
VD	233	1	9
I Tracker	192	2	16
O Tracker	180	5	36
RICHs	320	1	10
ECAL	10	5	2
HCAL	4	5	1
Muon	150	1	6
Trigger			1
TOTAL	$\sim$ 1100		$\sim$ 80

event building schemes, e.g. partial event building for the Level-2 algorithms, could reduce this rate significantly. If we compare these requirements with those of other LHC experiments, we believe that event building should not pose a serious problem.

7.3 The high level triggering

The first estimates of the processing power needed to implement the high-level triggers shows that the associated cost is a large fraction of the total cost of the DAQ system. In order to obtain more precise estimates of the CPU power, it is necessary to devise and understand the algorithms applied in the high level triggers.

The distinction between Level-2 and Level-3 is that the algorithms work only on partial event data, using the guidance provided by Level-0 and Level-1. In order to proceed towards a Level-2 strategy the following points will be studied:

- Definition of a first set of reference channels of B decays and their characteristics.
- Classification of the nature of the Level-1 accepted events.
- Definition of the discriminating quantities between event classes.
- Design of the algorithms and specification of the required detector information.

We expect that one of the rewarding approaches [12] will be to join up the high p_{T} trigger tracks in the spectrometer with the tracks in the silicon, and thus correlate the high p_{T} information with the information from the vertex trigger.

For Level-3 we assume that we require the full event data for doing a fast reconstruction and analysis of the decay chain in order to select the interesting B channels.

Table 3 summarises our current estimates of trigger rates and reductions, data volumes and processing needs for one possible running scenario. These will be updated as we progress in our studies of the Level-2 and Level-3 algorithms.

Table 3: Summary of trigger rates and processing needs for high level triggers for a possible running scenario (Level-2 accessing 25% of the event data).

	Level-2	Level-3	Reconstruction	Storage	Total
Input rate(kHz)	40	5	0.2	0.2	
Output rate(kHz)	5	0.2	0.2	0	
Reduction factor	8	25	1	1	
Execution needs(MI)	10	200	2000	10	
Data used(Kbytes/%)	20/25	60/75	80/100	120/150	
Network (GBytes/sec)	0.8	0.3	0	0.03	1.1
CPU Power(1000 MIPS)	400	1000	400	2	1800

7.4 Planned further studies

In 1997 we will perform the following studies:

- Analyse the detector front-end readout requirements.
- Develop the Level-2 strategy by first understanding the nature of events accepted by the Level-1 trigger,and then defining the discriminating quantities and algorithms. This to be followed by simulation of the algorithm performance.
- Develop event building and processor management models based on the requirements.
- Spreadsheet modelling using different scenarios for parameter values to obtain the requirements for items such as number of links, crates, buffers and cost.
- Data flow simulation of the most promising models to verify performance with respect to latencies, buffer occupancies, etc.

8 Major Milestones and Responsibilities

Each chapter of this document has outlined studies which are necessary to demonstrate the feasibility of the LHC-B Trigger/DAQ system for the Technical Proposal. The detailed work plan is given in the chart attached to the end of this document. Here we list the major milestones :

10 September 1997: A global trigger strategy will be defined for physics performance studies using the standard LHC-B detector simulation program.

3 October 1997: Detailed requirements for the front-end electronics for all the detectors will be specified.

1 December 1997: A baseline model for the LHC-B trigger and data acquisition system will be available, together with costings.

The Trigger work is convened by U. Straumann (Heidelberg) and S Conetti (Virginia), computing by J. Harvey (CERN) and DAQ by F Harris (Oxford/CERN). The following list indicates the current distribution of responsibilities:

- **Level-0**

  Simulation studies: M. Borkovski (PNPI), S. Conetti (Virginia), G. Corti (Virginia), B. Cox (Virginia) I. Korolko (ITEP), A. Tsarergorodtsev (PNPI/CERN), G. Wilkinson (CERN)

  Implementation studies: S. Conetti (Virginia), B. Cox (Virginia), D. Crosetto (Rice)

- **Level-1, vertex topology**

  Simulation studies: T. Bowcock (Liverpool), H. Dijkstra (CERN), W. Hoogland (NIKHEF), P. Koppenberg (U Lausanne), R. McNulty, T. Ruf (CERN), D. Steel (U Lausanne), L. Wiggers (NIKHEF), N. Zaitsev (NIKHEF)

  Implementation studies: J. Buytaert (CERN), B. Jost (CERN), P. Mato (CERN), H. Mueller (CERN), L. Wiggers (NIKHEF)

- **Level-1, tracking**

  Simulation studies: T. Hessing (Oxford) D. Hu (Heidelberg), P. Schleper (Heidelberg), U. Straumann (U Heidelberg)

  Implementation studies: M. Cuje (Heidelberg)

- **Level-2/Level-3**

  Simulation studies: J. Holt (Oxford), A. Nippe (Lausanne), P. Schleper (Heidelberg), C. Shepherd-Themistocleous (CERN)

- Front-end electronics and Trigger and Timing Control(TTC)

  Requirements analysis and baseline design: Y. Ermoline (Lausanne), H. Müller (CERN)

- **Data Acquisition**

  Requirements analysis, modelling and baseline design: J .-P. Dufey (CERN), F. Harris (Oxford/CERN), J. Harvey (CERN), B. Jost (CERN), P. Mato (CERN), H. Müller (CERN), L. Wiggers (NIKHEF)

References

[1] K. Krisebom et al. (The LHC-B collaboration), *LHC-B Letter of Intent*, CERN/LHCC 95-5, LHCC/I8, 1995.

[2] LHC-B Trigger/DAQ group, *Trigger and Data Acquisition Progress Report*, LHC-B 97-5, 1997

[3] G. Wilkinson, *LHC-B Hadron Trigger*, LHCB 96-3, 1996.

[4] S. Conetti and G. Corti, *LHC-B Electron Trigger*, LHCB 96-9, 1996.

[5] B. Cox and G. Corti, *LHC-B Muon Trigger*, LHCB 97-1, 1997.

[6] M. Borkovsky et al., *Study of the LHC-B Muon Trigger*, LHCB 97-7, 1997.

[7] D. Crosetto, *High Speed, Parallel, Pipelined processor architecture for front-end electronics and methods of use thereof*, LHC-B note LHCB 96-02, Feb 16, 1996.
D. Crosetto and S. Conetti, *Implementing Level-1 Trigger*, Proceedings of the IEEE Real Time 95 Conference, East Lansing, Michigan (May 1995).

[8] HERA-B T. Lohse et al. (The HERA-B collaboration), *Technical Design Report*, DESY-PRC 95/01, 1995.

[9] P. Lichard,*The ATLAS TRT Readout system*,Second Workshop on Electronics for LHC Experiments, CERN/LHCC/96-39, 21 October 1996, pp. 442.

[10] N. Zaitsev et al., *Status Report on the development of the primary vertex fast reconstruction*, Nikhef,January, 1997.

[11] H. Müller et al., *Ideas on a 1st level r-ϕ vertex trigger processor*, LHCB 97-6, 1997.

[12] G. Wilkinson, *Investigations into impact parameter triggers seeded from Level 0 hadron trigger input*, LHCB 96-11, 1996.

[13] Y. Ermoline, *LHC-B requirements for TTC*, Proceedings of TTC Workshop, CERN, October, 1996.

LHC-B Trigger / DAQ Workplan for 1997 (I)

ID	Task Name
1	**L0/L1 Trigger Simulation**
2	**Update LHC-B simulation package**
3	**Level0 trigger (electron, Muon, Hadron)**
4	**Level1 Trigger**
5	Vertex (Detector simulation)
6	Vertex (Trigger simulation)
7	Tracking
8	**Overall Steering**
9	**L0/L1 algorithms specified**
10	**Tuning of L0/L1 trigger algorithms**
11	**Optimize cuts of L0 algorithms**
12	**Tune tracking trigger**
13	**Vertex trigger**
14	Tune algorithm for acceptance and background
15	Optimize detector geometry
16	Study impact of detector misalignment
17	Study impact of detector/electronic noise
18	Study impact of pile-up events
19	**L2 trigger**
20	Define first set of reference channels and their characteristics
21	Study nature of L1 accepted events
22	Define discriminating quantities
23	**Simulate algorithms (including detector information needec**
24	Matching vertex detector with tracking
25	**L2 algorithms specified**
26	**L3 trigger**
27	Estimate requirements for L3 (fast reconstruction)
28	**Global trigger strategy available for physics studies**
29	**DAQ studies**
30	Event filter processing requirements
31	Event builder studies
32	Study parameterized model of DAQ system (incl. costing)
33	Develop simulation tools
34	Develop behavioral models
35	Simulate models
36	**Baseline DAQ model**

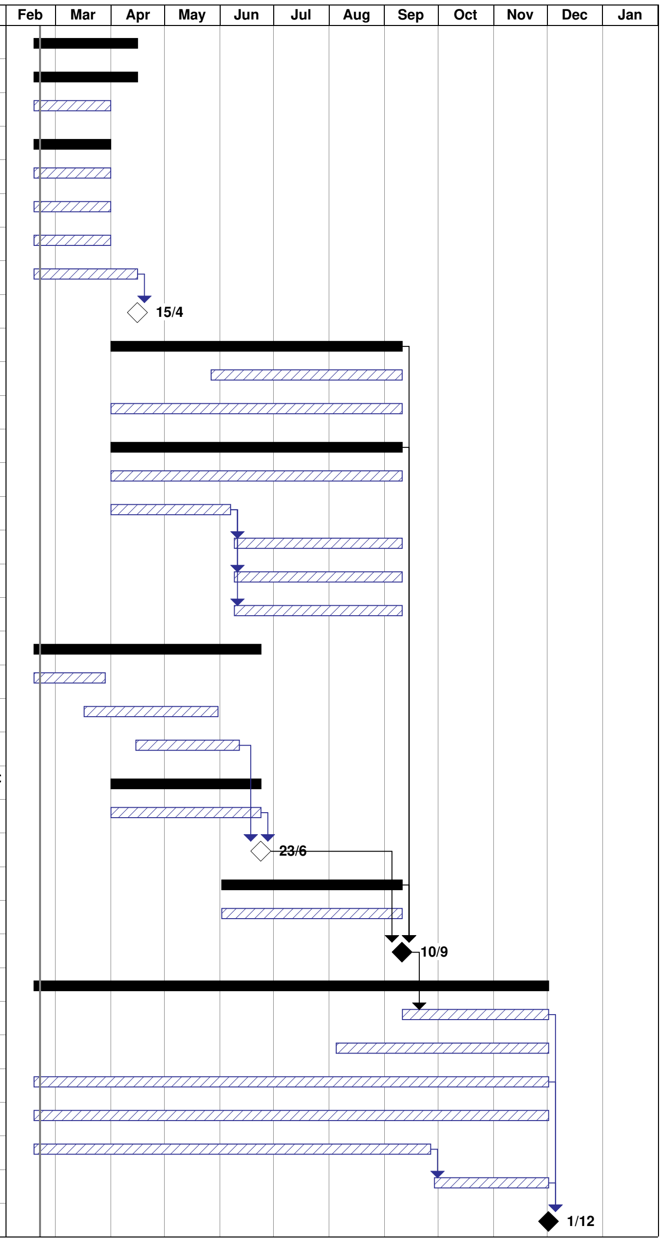

LHC-B Trigger / DAQ Workplan for 1997 (II)

ID	Task Name
37	**Trigger implementation studies**
38	**L0 implementation studies ('3d-flow')**
39	Prototype production (40 pieces)
40	Assemble prototype system
41	Test with Calorimeter
42	Evaluation of tests
43	Evaluation report
44	**Evaluation of silicon barrel detector**
45	Study silicon barrel detector
46	**Decide on silicon barrel detector**
47	**Vertex Trigger implementation feasibility studies**
48	Trigger input data extraction studies
49	Data processing studies
50	Development of baseline model
51	Verify feasibility of critical components
52	Vertex trigger baseline implementation model
53	**Track trigger implementation studies**
54	Studies based on HERA-B designs
55	Track trigger baseline implementation model
56	**Trigger baseline implementation model**
57	**Vertex detector studies**
58	Vertex Detector prototype production
59	Hybrid design, production, tests
60	Detector assembly, lab tests
61	Vertex detector beam tests
62	Evaluation of detector performance
63	Studies on environmental/mechanical problems (cooling,...)
64	**Preliminary conclusion on detector performance**
65	**Front-end electronics studies**
66	Collect FE requirements for each detector
67	Define common FE model
68	Study each detector within common framework
69	Understand requirements for TTC to FE
70	**Produce FE requirements specification report**